nutraceuticals

MDPI

Article

Pharmacokinetic Evaluation of Oleuropein from the Olive Tree (*Olea europaea*)

Pradeep Subedi [1], Rocío Rivera Rodríguez [2], Pariksha Thapa [2], Daniel Lantvit [2] and Jeremy James Johnson [1,*]

[1] Department of Pharmacy Practice, Retzky College of Pharmacy, University of Illinois Chicago, Chicago, IL 60612, USA; subedi@uic.edu
[2] Department of Pharmaceutical Sciences, Retzky College of Pharmacy, University of Illinois Chicago, Chicago, IL 60612, USA; rriver49@uic.edu (R.R.R.); pthapa6@uic.edu (P.T.); lantvit@uic.edu (D.L.)
* Correspondence: jjjohn@uic.edu; Tel.: +1-312-996-4368

Abstract

In this study, the pharmacokinetic (PK) characteristics of oleuropein present in the olive tree (*Olea europaea*) were determined. We developed and validated a highly sensitive ultra-performance liquid chromatography coupled with tandem mass spectrometry (UPLC-MS/MS) method to quantify oleuropein and its aglycone derivative, thereby establishing their pharmacokinetic properties in vitro and in vivo. Quantification of oleuropein and oleuropein aglycone was performed using selected reaction monitoring (SRM) with heated electrospray ionization in negative ion mode, employing mass transitions of m/z 275.06 and 307.137 for the respective analytes, and methylparaben as the internal standard. The calibration curve for both exhibited a range from 1 ng/mL to 1000 ng/mL, utilizing a total of 10 calibrator standards. The method demonstrated superior sensitivity, precision, and reproducibility, facilitating accurate quantification of analytes over a wide concentration range in biological matrices. To develop a pharmacokinetic profile, C57BL/6 male mice were administered oleuropein at a dose of 100 mg/kg body weight via oral gavage, and plasma levels were examined by LC-MS/MS. Oleuropein pharmacokinetics were evaluated exclusively, as plasma levels of oleuropein aglycone remained below the limit of quantification throughout the 24 h sampling period. Mass analysis of plasma samples identified multiple glucuronidated and sulfated metabolites, establishing Phase II metabolism as the dominant pathway governing the systemic disposition of oleuropein. In addition, the metabolic stability of the compounds was also investigated in mouse liver microsomes and S9 fractions to define the in vivo stability of oleuropein and oleuropein aglycone.

Keywords: oleuropein; oleuropein aglycone; olive oil; pharmacokinetics; olive leaf

Received: 27 December 2025
Revised: 11 February 2026
Accepted: 1 April 2026
Published: 13 April 2026

1. Introduction

The olive tree (*Olea europaea* L.) is a defining species of the Mediterranean basin, historically revered for its nutritional and medicinal offerings. Its fruits and oil are central to the Mediterranean diet, a dietary pattern associated with a reduced incidence of chronic diseases [1,2]. This protective effect is primarily attributed to a suite of bioactive phenolic compounds intrinsic to the olive matrix. Among these, the secoiridoid glycoside oleuropein is the most abundant and characteristic constituent, found in high concentrations in olive leaves and fruit [3]. In addition, these phytochemicals are popular as ingredients in dietary supplements and nutraceuticals. The traditional use of olive leaf extracts in folk medicine for ailments ranging from fever to microbial infections presaged modern scientific

interest, which now identifies oleuropein as a principal mediator of these broad therapeutic properties [4]. Its chemical structure, featuring a hydroxytyrosol moiety linked to elenolic acid via a glucose molecule, renders it a pivotal precursor to a range of bioactive metabolites (Figure 1). This prodrug nature fundamentally dictates its biological activity in vivo, setting the stage for a complex pharmacological profile that integrates potent antioxidant, anti-inflammatory, and modulatory effects on key cellular pathways [5]. Thus, oleuropein stands as a critical phytochemical linking traditional wisdom to contemporary nutraceutical and pharmacological research.

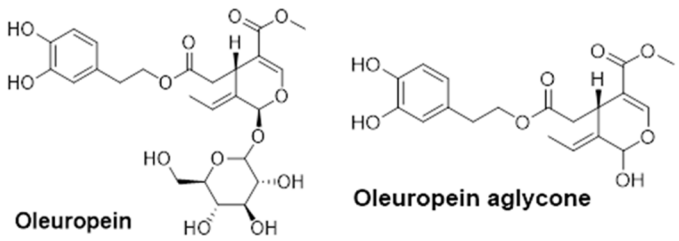

Figure 1. Chemical structure of oleuropein and oleuropein aglycone.

Oleuropein and its metabolites exert pleiotropic effects through integrated antioxidant and anti-inflammatory pathways. They function as free radical scavengers and metal ion chelators, diminishing lipid peroxidation and reactive oxygen species (ROS) while enhancing endogenous defenses such as superoxide dismutase (SOD) and catalase [6–8]. This effectively inhibits LDL oxidation, a crucial factor in atherogenesis [4,9]. They also control chronic inflammation by blocking the NF-κB pathway, which lowers adhesion molecules like VCAM-1 and pro-inflammatory cytokines like TNF-α and IL-6 [10–12]. Oleuropein systematically addresses metabolic syndrome through hypolipidemic and anti-obesity effects. By activating AMPK and downregulating PPARγ and C/EBPα, it prevents adipogenesis [13,14]. Its hypoglycemic efficacy arises from AMPK-mediated GLUT4 translocation and α-glucosidase inhibition [14–16]. Additionally, by inhibiting amyloid-β aggregation and triggering autophagy through the AMPK/mTOR axis, it provides neuroprotection [4,17]. Oleuropein aglycone has enhanced bioactivity, disrupting protein clumps and causing death in malignant cells [18]. Ultimately, its antimicrobial and antiviral activity entails the disruption of microbial lipid bilayers [19].

The pharmacokinetic profile of oleuropein is determined by rapid metabolic changes that necessitate accurate in vitro evaluation. Phase I microsomal esterases are involved in the hydrolysis of oleuropein to its aglycone form, whereas the biosynthetic and degradative routes encompass intricate transitions mediated by β-glucosidase [20]. The incorporation of Phase II enzymatic pathways, namely glucuronidation and sulfation, is essential, as these high-capacity systems efficiently sequester metabolites immediately upon their synthesis [21,22]. Prior studies have often concentrated on intestinal absorption but generally omit the precise Phase II activity data usually obtained from hepatic S9 fractions [23]. Assessing metabolic stability by microsomal and S9 assays enables the identification of the principal enzymatic barriers that restrict the bioavailability of the parent molecule [24]. A primary obstacle in secoiridoid research remains the disconnect between in vitro potency and in vivo detectable efficacy. Although oleuropein aglycone is often recognized as a powerful, lipophilic contributor to health benefits, its real presence in systemic circulation is inadequately understood owing to its conversion to hydroxytyrosol during numerous metabolic processes [25,26]. This inconsistency primarily arises from the chemical instability of oleuropein aglycone and the absence of high-sensitivity, proven analytical techniques capable of differentiating between the parent secoiridoid and its ephemeral intermediates in intricate biological matrices [27,28]. Therefore, there is an immediate need to evaluate

the pharmacokinetics of the aglycone using established LC–MS/MS methods to determine the extent of its systemic exposure [29,30].

Despite the recognized therapeutic potential of oleuropein and its bioactive aglycone, a critical knowledge gap persists regarding their pharmacokinetic profiles in mice. This is especially important as mouse models are routinely used to evaluate the biological activities of phytochemicals, including oleuropein and oleuropein-containing plant extracts. The present research fills existing gaps by studying oleuropein pharmacokinetics with a newly validated LC-MS/MS approach that simultaneously quantifies oleuropein and oleuropein aglycone in vivo. Significantly, we expanded this investigation to plasma samples to examine the systemic metabolite profile of oleuropein. Supported by in vitro stability assays in liver microsomes and S9 fractions, this integrated approach establishes a grounded pharmacological framework for oleuropein in preclinical research.

2. Materials and Methods

2.1. Chemicals and Reagents

Oleuropein and oleuropein aglycone were obtained from Medchem Express (Monmouth Junction, NJ, USA). Water (Optima LC-MS grade; w6-4), acetonitrile (Optima LC-MS grade; A955-212), methanol (Optima LC-MS grade; A456-4), and formic acid (Optima LC-MS grade; A117) were purchased from Fisher Scientific (Fair Lawn, NJ, USA). The LC analytical column and guard column were obtained from Phenomenex (Torrance, CA, USA).

2.2. Instrumentation and LC-MS/MS Conditions

The liquid chromatography system consisted of a Thermo Fisher Scientific Vanquish Binary pump, a Base Vanquish Horizon system, and a Split Sampler FT (West Palm Beach, FL, USA). The chromatographic system was coupled to a triple-stage quadrupole mass spectrometer (Quantis) from Thermo Fisher Scientific, equipped with a heated electrospray ionization (H-ESI) probe. The separation of the analytes was conducted using a Kinetex C18 3 mm × 50 mm, 2.6 µM analytical column (Phenomenex, USA), with an attached guard column (SecurityGuard EVO-C18 2 mm × 3 mm, part no. AJ0-9297; Phenomenex, USA). The mobile phase used for chromatography is composed of solvent A (0.1% formic acid in HPLC-grade water) and solvent B (0.1% formic acid in acetonitrile). The percentage of solvent B used was as follows: 10% (0 to 0.2 min), 95% (0.2 to 3.3 min), 95% (3.3 to 3.7 min), 10% (3.7 to 4.0 min), and 10% (4.0 to 5.0 min), with a flow rate of 0.35 mL/min. The column was maintained at a constant temperature of 40 °C, and the autosampler was set to 4 °C. The mass spectrometry conditions were as follows: H-ESI in negative mode, with a spray voltage of 4236.36 V; sheath gas at 20.9 arbitrary units (Arb); and auxiliary gas at 22.8 Arb. Further details regarding the MS conditions are provided in Table 1.

Table 1. Mass spectrometric ion source and instrument operating parameters for oleuropein and oleuropein aglycone.

Instrument Parameter	Operating Condition
Ion Source Type	H-ESI
Spray Voltage	Static
Positive Ion (V)	4236.36
Sheath Gas (Arb)	20.9
Auxiliary Gas (Arb)	22.8
Sweep Gas (Arb)	1.2
Ion Transfer Tube (°C)	300
Vaporizer Temp (°C)	350
Polarity	Negative

Table 1. *Cont.*

Instrument Parameter	Operating Condition
Dwell Time (ms)	40
Q1 Resolution (FWHM)	0.7
Q3 Resolution (FWHM)	0.7
CID Gas (mTorr)	1.5

2.3. Analytical Standards and Sample Preparation

The stock solutions of oleuropein and oleuropein aglycone, hereafter both referred to as the analyte, and the internal standard (methyl paraben) were prepared in methanol to a final concentration of 1 mg/mL. Methylparaben (MP) was selected as the internal standard due to its structural and ionization compatibility with secoiridoid analytes, sharing both phenolic and ester functional groups. MP ensures stable recovery and elution in regions free from ion suppression. In preference to isotope-labeled oleuropein, which is commercially limited and undergoes complex metabolic cleavage at multiple sites, accurate tracking is challenging.

The desired serial concentrations of working solutions were achieved by diluting a stock solution of the analyte with methanol. Blank plasma was spiked with an appropriate volume of internal standard to generate the blank plasma samples. Then, 5 µL of working solution was added to 25 µL of blank plasma samples to prepare calibration plasma samples at concentrations ranging from 1 to 1000 ng/mL (1, 2.5, 5, 10, 25, 50, 100, 250, 500, and 1000 ng/mL). Three quality control (QC) samples consisting of blank plasma samples spiked with known concentrations of the analyte (25 ng/mL, 100 ng/mL, and 500 ng/mL) were prepared independently from those used for the calibration curve. These QC samples were prepared on the day of analysis in the same way as the calibration standards. All the stock and working solutions were stored at −80 °C before and after use.

2.4. Blood Sample Collection

Thirty-six C57BL/6 male mice were acquired from Jackson Laboratories (Bar Harbor, ME, USA). At 6 weeks of age, mice were housed in plastic cages and received standard chow (AIN-76) and water *ad libitum* prior to the experiment. Mice were housed and maintained on a 12 h/12 h light/dark cycle. All the mice were weighed and dosed accordingly with freshly prepared oleuropein at 100 mg/kg body weight. Animal experiments were performed according to the policies and guidelines of the Institutional Animal Care and Use Committee (IACUC) of the University of Illinois Chicago. Mice were euthanized in accordance with Institutional Animal Care and Use Committee approval (protocol 22-165; approved on 12 May 2022) and current American Veterinary Medical Association (AVMA) guidelines (2020) using CO_2 introduced by gradual fill (30–70% chamber volume/min); animals were observed until respiratory arrest, CO_2 flow was continued for ≥1–2 min, and death was confirmed by an AVMA-approved secondary physical method.

Whole blood samples from four mice at each time point were collected via submandibular puncture at 0, 0.25, 0.5, 1, 2, 4, 6, 12, and 24 h following the administration of oleuropein. These blood samples were collected in lithium heparin-coated tubes, centrifuged at 3000 rpm for 15 min at 4 °C, and the resulting plasma was transferred to microcentrifuge tubes and stored at −80 °C for subsequent analysis.

2.5. Plasma Processing

Blank plasma samples (45 µL) were transferred into appropriately labeled 1.5 mL microcentrifuge tubes. Calibration and QC plasma samples were prepared by adding 5 µL of calibration standard or QC working solution to the blank plasma samples. Blank

plasma samples contained the internal standard solution, whereas double-blank samples contained neither the analyte nor the internal standard; instead, 5 µL of methanol was added to compensate for them. For study samples, 50 µL of plasma was aliquoted into microcentrifuge tubes. Protein precipitation was performed by adding 150 µL of acetonitrile, followed by vortex mixing. All samples were centrifuged at 16,000× *g* for 30 min, and the supernatant was transferred to labeled tubes. The supernatant was evaporated to dryness under a gentle stream of nitrogen at room temperature, protected from direct light. The residue was reconstituted with 100 µL of acetonitrile–water (80:20, *v*/*v*), and 50 µL was transferred to autosampler vials. A 5 µL aliquot was injected into the LC–MS system for analysis.

2.6. LC-MS/MS Data Analysis

Data were analyzed with Tracefinder 5.1 SP3 software (Thermo Fisher Scientific, Waltham, MA, USA). Calibration curves were established with the calibration standards prepared in blank plasma. The calibration curve of oleuropein and oleuropein aglycone was best described by a $1/X^2$ weighted linear regression of the peak area ratio in each standard sample.

2.7. LC-MS Method Validation

Validation was conducted to assess the performance of the method in accordance with the recommendations published by the U.S. Food and Drug Administration (FDA). The selectivity of the process was investigated to identify any interference at the retention time of the analyte and internal standard originating from plasma or other sources. This was determined by comparing blank plasma with the blank plasma spiked with the analyte and internal standard.

Carryover was estimated by injecting a blank plasma sample immediately after the highest concentration (1000 ng/mL) of the calibration standard was injected. Carryover was considered acceptable when the analyte concentration was below 20% of the lower limit of quantification (LLOQ). Extraction recovery and matrix effect were evaluated at QC levels. Extraction recovery was calculated by comparing the peak area ratio (analyte/internal standard) of samples spiked before extraction with those spiked after extraction. The matrix effect was determined by comparing the peak area ratio of post-extraction spiked samples with neat standard solutions prepared in the solvent at equivalent concentrations. Intra-day precision and accuracy were evaluated using three replicates of quality control samples at concentrations of 500 ng/mL, 100 ng/mL, and 25 ng/mL. Inter-day precision and accuracy were assessed on three different days. Precision was calculated as the coefficient of variation (CV, %) within a single run (intra-run) and between different extractions and runs (inter-run).

The stability of oleuropein and oleuropein aglycone was investigated at room temperature (RT), 4 °C, −80 °C, and under multiple freeze–thaw cycles. Blank plasma samples spiked with oleuropein and oleuropein aglycone were stored at RT and 4 °C for 24 h prior to analysis. Long-term storage at −80 °C was also assessed over a six-month period. Multiple freeze–thaw cycles were conducted by thawing the sample on ice for 1 h, followed by storage at −80 °C for 23 h each day, for up to ten cycles.

2.8. Pharmacokinetic Analysis

Plasma samples for pharmacokinetic analysis were collected at 0, 0.25, 0.5, 1, 2, 4, 6, 8, and 24 h. From plasma time-concentration data, maximum observed plasma concentration (C_{max}), time at observed maximum concentration (T_{max}), area under plasma concentration (AUC), and terminal elimination half-life ($t_{1/2}$) of oleuropein and oleuropein aglycone were calculated. Mean plasma concentration versus time at various sampling times was

analyzed using standard non-compartmental methods with Phoenix WinNonlin (version 6.3; Certara, Princeton, NJ, USA). The linear-up–log-down rule estimated the AUC from time zero to the last measured concentration.

2.9. Stability in Mouse Plasma

Frozen plasma was thawed in a room-temperature water bath. It was then centrifuged at 3200× *g* for 10 min to remove clots. The supernatant was collected into a fresh tube. Only plasma thawed no more than twice since arrival was used.

Working solutions of oleuropein and oleuropein aglycone were prepared at a concentration of 1 mM. First, 4 µL of the working solution was added to 796 µL of pre-incubated plasma to achieve a final concentration of 5 µM. The solvent concentration in the final mixture was 0.5%. For each time point (5, 15, 30, 60, and 120 min), 50 µL aliquots of the spiked plasma were transferred into new tubes and incubated in a 37 °C water bath. Then, 400 µL of chilled quench solution (methanol with internal standards) was added to the spiked plasma at the designated time points to stop the reaction. For time 0 samples, 50 µL of the spiked plasma was added to tubes containing 400 µL of the quench solution. The samples were vortexed for 5 min and centrifuged at 10,000× *g* for 30 min at 4 °C to precipitate the proteins. The supernatant was collected for analysis via LC-MS/MS. The assay was performed in duplicate.

2.10. Metabolic Stability in Pooled Male Mouse Liver Microsomes/S9 Fraction

Frozen microsomes and the S9 fraction were thawed in an ice bath. Only those microsomes and S9 fractions that had been thawed no more than five times since arrival were used. Two separate experiments were conducted with and without cofactors to determine metabolic stability. For the assay with the cofactors, the incubation system included 0.5 mg/mL of microsomal or S9 fraction, 2 mM uridine 5′-diphosphate-glucuronic acid (UDPGA), 2.5 mM glutathione, an NADPH regeneration system (comprising 0.5 mM NADP+, 2 mM glucose 6-phosphate, 5 mM $MgCl_2$, and 0.2 units/mL Glucose-6-phosphate dehydrogenase (G6PDH)), and 20 µg/mg of alamethicin in a total volume of 50 µL of 100 mM phosphate buffer at pH 7.4. A separate experiment was conducted, without any cofactors, using only the microsomal or S9 fraction and the test compound in a total volume of 50 µL of 100 mM phosphate buffer at pH 7.4. The reaction was initiated by adding the test compound to reach a final concentration of 1.0 µM, followed by incubation at 37 °C. At each point (5, 15, 30, 60, and 120 min), the reaction solutions were stopped by adding cold acetonitrile containing internal standards (IS). For time 0 samples, the reaction mixture was added to tubes containing the quench solution. The samples were vortexed for 5 min and then centrifuged at 10,000× *g* for 30 min at 4 °C to precipitate the proteins. The supernatant was collected for analysis via LC-MS/MS. The assay was performed in duplicate.

Intrinsic clearance (CL_{int}) was determined from the depletion of the parent compound during incubation. The natural logarithm of the percentage of parent compound remaining was plotted against incubation time, and the elimination rate constant (k) was obtained from the slope of the linear regression (k = −slope). The in vitro half-life ($t_1/_2$) was calculated using $t_1/_2 = 0.693/k$, and intrinsic clearance (CL_{int}, µL/min/mg protein) was calculated by multiplying k by the incubation volume (µL) and dividing by the amount of protein (mg), using the mean of duplicate measurements.

2.11. Statistical Analysis

Pharmacokinetic parameters were calculated using non-compartmental analysis (NCA). Statistical analyses were performed using GraphPad Prism 10 software (GraphPad Software, San Diego, CA, USA). Data from nine independent groups were subjected to one-way ANOVA followed by a post hoc analysis with Tukey's test to determine significant

differences among groups. Differences at $p < 0.05$ were considered statistically significant. Results are presented as mean values ± SD.

3. Results

3.1. LC-MS/MS Optimization

Tuning and optimization of the analytes were achieved by direct injection of individual solutions at a concentration of 1000 ng/mL into the MS/MS detector, with mobile phases A and B run at a flow rate of 0.5 mL/min in a 50:50 (*v*/*v*) mixture. SRM transitions and collision energy of the analyte and internal standard are reported in Table 2. Two transitions, one for quantification and the other for confirmation, were selected for the analytes and internal standard to improve the assay's specificity.

Table 2. Optimized MS/MS transitions and mass spectrometric parameters for oleuropein and oleuropein aglycone (analyte) and methyl paraben (internal standard).

Analyte	Retention Time (min)	Precursor Ion	Product Ion (Quantifier)	Collision Energy (V)	Product Ion (Qualifier)	Collision Energy (V)	RF Lens (V)
Oleuropein	2.7	539.29	275.065	20.54	223.125	22.44	173
Oleuropein aglycone	2.7	377.25	307.137	9.21	275.083	9.97	105
Methyl-paraben	2.7	151.162	136.071	12.79	92	18.86	76

3.2. Calibration Curve and Quantification

Quantification of oleuropein and oleuropein aglycone was performed using the internal standard method. The calibration curve was best described by a $1/X^2$ weighted linear regression of the peak area ratio in each standard sample. The assay proved linear and acceptable, as the regression coefficients were greater than 0.99.

3.3. Method Validation

The developed LC-MS/MS procedure for oleuropein and oleuropein aglycone quantifications was validated in accordance with the instructions and recommendations described in Section 2. QC samples at low (LQ), medium (MQ), and high (HQ) concentration levels were used to verify the linearity, accuracy, precision, and extraction efficiency of the procedure. The detailed results are shown in Table 3.

Table 3. Accuracy and precision of oleuropein and oleuropein aglycone spiked into blank mouse plasma at low, mid, and high QCs. Inter-day and intra-day accuracy and precision were tested using three replicates at each QC concentration, with the experiment performed on three separate days.

	QC's	Concentration (ng/mL)	Accuracy		Precision		Extraction Recovery (%)
			Intra-Day (%)	Inter-Day (%)	Intra-Day (%)	Inter-Day (%)	
Oleuropein	LQ	25	95.46 ± 3.16	94.92 ± 4.37	13.62 ± 2.01	11.94 ± 1.6	94.79 ± 5.29
	MQ	100	94.83 ± 2.46	95.27 ± 3.47	10.58 ± 2.73	6.73 ± 1.04	
	HQ	500	97.28 ± 3.33	97.18 ± 2.09	9.03 ± 1.33	8.25 ± 4.23	
Oleuropein aglycone	LQ	25	95.16 ± 4.31	96.19 ± 3.21	5.39 ± 3.02	9.86 ± 2.36	95.85 ± 3.87
	MQ	100	97.25 ± 2.35	94.29 ± 2.09	7.19 ± 1.94	8.42 ± 2.69	
	HQ	500	98.03 ± 2.35	97.32 ± 2.09	10.45 ± 2.29	11.27 ± 1.03	

The linearity of the method was evaluated through internal standard calibrations. The calibration curves for each were established using a $1/X^2$ weighted least squares fit, achieving correlation coefficients (R^2) of 0.99 or higher. The measured concentrations for all calibration levels closely aligned with nominal values, and the accuracy was maintained within 15% for all analytes. The method exhibited high reliability and reproducibility for both analytes. All measured values for intra-day and inter-day accuracy and precision adhered to the established acceptance criteria of ±15% deviation from the nominal concentration and ±15% RSD. The results of selectivity and specificity testing indicated no interference with the analyte or internal standard from endogenous impurities or other agents. All analyte and internal standard peaks exhibited identical transitions and retention characteristics. No analytes were detected in the reagents or water tested. The blank samples showed no endogenous interference at the retention times corresponding to each analyte.

The matrix effect was quantitatively assessed by comparing the peak areas of analytes spiked into post-extracted plasma to those in pure solvent. For oleuropein and oleuropein aglycone, the mean matrix factors were 91.4% and 93.7%, respectively, with a coefficient of variation (CV) of <5.1% across three different plasma lots (Supplementary Material Table S1). The IS-normalized matrix factors remained between 0.95 and 0.98, demonstrating that methylparaben effectively accounts for ion suppression in the plasma matrix, ensuring high analytical consistency.

Oleuropein and oleuropein aglycone demonstrated high accuracy and precision, with mean values across QC levels and days ranging from 94.83% to 98.03% and 6.73% to 13.62%, respectively. The sample preparation procedure demonstrated robustness and consistency, with mean extraction recoveries of 94.79% for oleuropein and 95.85% for oleuropein aglycone, respectively.

The stability of oleuropein and oleuropein aglycone was thoroughly evaluated under different storage and handling conditions (Figure 2). The findings, presented as the mean percentage change relative to the standard concentration, are displayed in Table 4 (Supplementary Tables S2–S4). The criterion for acceptance regarding stability was established as a mean percentage change of ±15%. The method exhibited satisfactory stability of the autosampler in both cases. All re-injected QC samples after 6 h exhibited minimal deviation, with variations remaining within the acceptable range, thereby confirming stability throughout the analytical batch duration. The results of the short-term bench-top stability test (24 h at room temperature) indicated that both remained stable at room temperature. Refrigeration at 4 °C for 24 h significantly enhanced the stability of both compounds. After 24 h, only 10% and 13% degradation was observed for oleuropein and oleuropein aglycone, respectively. Storage at −80 °C for six months resulted in only a 12% and 14% degradation of oleuropein and oleuropein aglycone, respectively, demonstrating the efficacy of this storage condition. The stability of the samples under repeated freeze–thaw stress was assessed by quantifying the residual percentage of oleuropein and oleuropein aglycone across multiple cycles. The rate of decline exhibited a gradual initial loss, which then increased steadily from the fourth cycle (8%) to the tenth cycle (11%). During the testing period, the stability profiles of oleuropein and oleuropein aglycone exhibited similar patterns of decline.

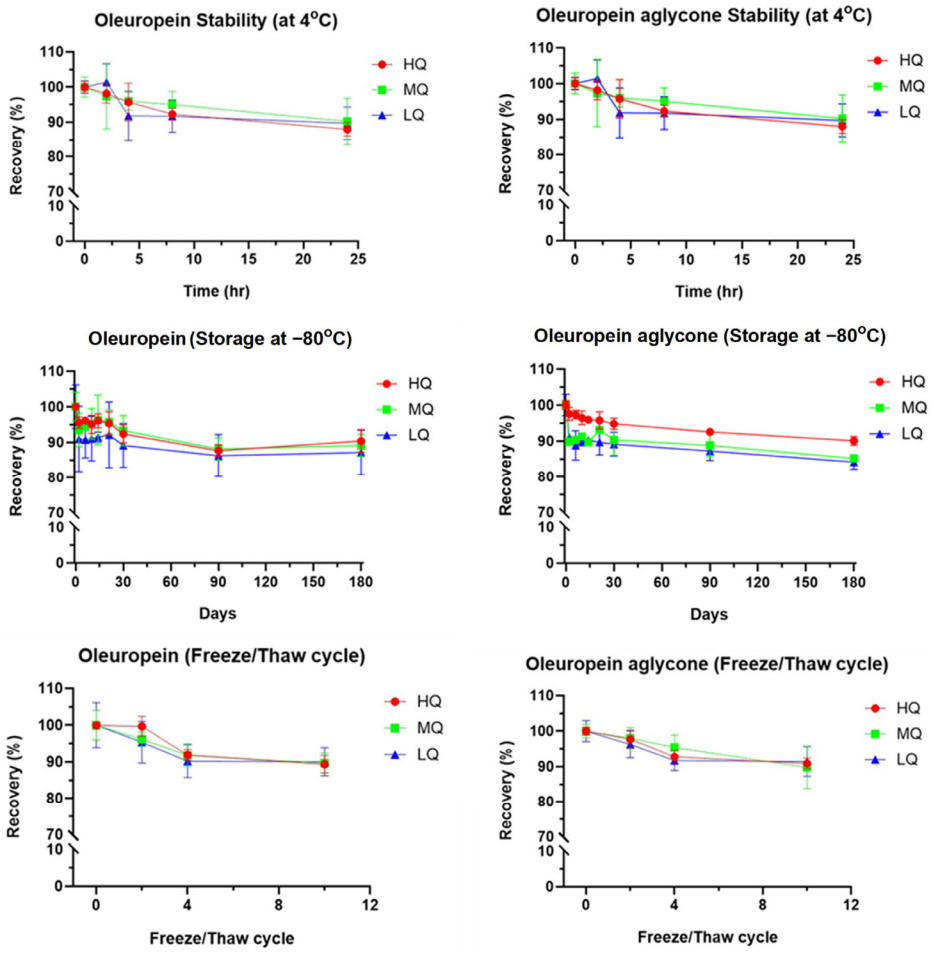

Figure 2. Stability of oleuropein and oleuropein aglycone at room temperature (RT), 4 °C, 6-month storage at −80 °C, and multiple freeze–thaw cycles. HQ, MQ, and LQ refer to high-, medium-, and low-quality control (QC) samples.

Table 4. Stability of oleuropein and oleuropein aglycone at room temperature (RT), 4 °C, multiple freeze–thaw cycles, and 6-month storage at −80 °C. The stability was calculated as a percentage using three different concentrations of the samples. The stability was investigated over 48 h for samples stored at 4 °C and −80 °C. HQ, MQ, and LQ refer to high-, medium-, and low-quality control (QC) samples.

	QC'S	Concentration (ng/mL)	Stability (%) After 24 h at		Freeze–Thaw (10 Cycles)	−80 °C (6 Months)
			RT	4 °C		
Oleuropein	LQ	25	75.26 ± 4.83	89.69 ± 4.6	90.08 ± 3.85	86.23 ± 5.38
	MQ	100	78.53 ± 5.62	90.24 ± 6.57	89.69 ± 2.65	89.34 ± 4.64
	HQ	500	80.91 ± 3.29	88.01 ± 1.94	89.39 ± 2.4	90.22 ± 1.24
Oleuropein aglycone	LQ	25	72.04 ± 6.47	86.09 ± 1.65	91.48 ± 4.21	85.84 ± 1.83
	MQ	100	75.63 ± 4.21	87.78 ± 3.67	89.8 ± 5.96	86.41 ± 0.1
	HQ	500	74.35 ± 4.74	85.99 ± 1.61	90.91 ± 1.55	90.12 ± 1.32

3.4. Metabolic Stability of Oleuropein and Oleuropein Aglycone in Mouse Liver Microsomes and S9 Fractions

The metabolic stability of oleuropein and oleuropein aglycone was assessed in mouse liver microsomes and S9 fractions, both in the presence and absence of an NADPH-regenerating system (Figure 3, Supplementary Tables S5 and S6). Metabolism was predom-

inantly NADPH-dependent, indicating that Phase I cytochrome P450-mediated enzymatic pathways were primarily responsible for most of the observed turnover.

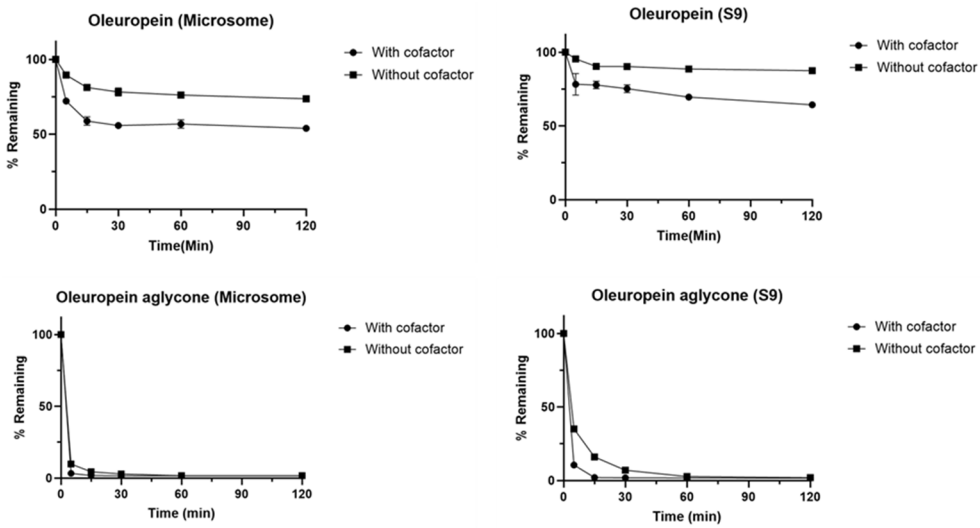

Figure 3. Metabolic stability profiles of oleuropein and oleuropein aglycone. Data represent the percentage of parent compound remaining over a 120-minute incubation period in mouse liver microsomes and S9 fractions, both in the presence and absence of metabolic cofactors. Each point represents the mean of duplicate determinations.

In mouse liver microsomes with cofactors, oleuropein aglycone was extremely unstable, showing a rapid decline to 3% remaining at 5 min. Oleuropein exhibited slower turnover, retaining 54% of its initial amount at 120 min. In the absence of cofactors, oleuropein was found to be more stable. After 120 min, 74% of oleuropein remained, whereas oleuropein aglycone continued to display notable non-NADPH-dependent degradation, falling to 1%. In S9 fractions, metabolic turnover proceeded more slowly than in microsomes but showed a similar pattern. With cofactors, 64% of oleuropein and only 1% of oleuropein aglycone remained at 120 min. Without cofactors, oleuropein remained highly stable (87% at 120 min), while oleuropein aglycone again showed extensive metabolism, with only 1% of the parent compound detectable. Overall, the data demonstrate that the metabolic clearance of both compounds is strongly cofactor-dependent, with microsomes exhibiting more rapid catalytic activity than S9 fractions.

The metabolic stability revealed a striking difference in the turnover rates of the two analytes across hepatic fractions. The calculated CL_{int} for the oleuropein aglycone was approximately 14-fold higher than that of the parent oleuropein in mouse liver microsomes. A similar trend was observed in the S9 fractions (Supplementary Table S7). The marked reduction in CL_{int} observed in the 'No cofactor' groups across both microsomal and S9 fractions highlights the predominant role of enzyme-mediated pathways in the rapid turnover of these phenolics.

3.5. Pharmacokinetics of Oleuropein

The mean pharmacokinetic parameters for oleuropein are summarized in Table 5 and Figure 4. Oleuropein exhibited rapid absorption, reaching its peak concentration within 30 min after a dose of 100 mg/kg was administered via oral gavage to mice. A C_{max} of 0.00835 µmol/mL confirmed efficient uptake, while the AUC values (0.0141 for $AUC_{0–24}$ and 0.0143 for $AUC_{0–inf}$) indicated that most exposure occurred within the sampling period. With an elimination half-life of 0.780 h, the data suggest a swift rise in concentration followed by a steady, predictable decline.

Table 5. Summary of pharmacokinetic parameters of oleuropein following a single oral administration in mice. Data are calculated from plasma concentration–time profiles over a 24-h period and are presented as mean ± SD (n = 4).

	C_{max} (μmole/mL)	T_{max} (h)	AUC_{0-t} (h × (μmole/mL))	AUC_{0-inf} (h × (μmole/mL))	Half Life (h)
Oleuropein	0.00835 ± 0.00088	0.5	0.0141 ± 0.00134	0.0143 ± 0.00135	0.780 ± 0.090

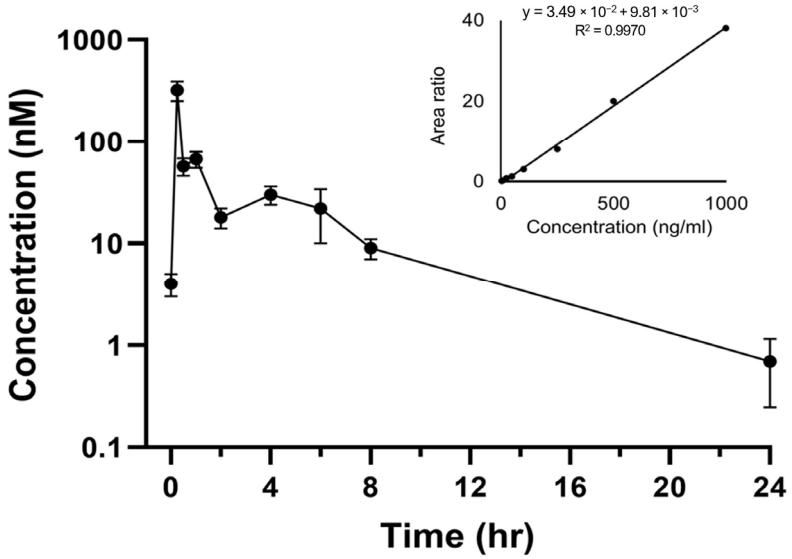

Figure 4. Semi-logarithmic plasma concentration–time profile of oleuropein following oral administration in mice. The primary plot illustrates the mean plasma concentration (ng/mL) over a 24 h period (mean ± SD, n = 4). The inset displays the representative calibration curve used for quantification, demonstrating linearity over the dynamic range of 1–1000 ng/mL.

3.6. Plasma Metabolite Profiling of Oleuropein

To elucidate the mechanistic basis underlying the metabolic instability of oleuropein, plasma samples were analyzed by LC–MS/MS (Table 6). Oleuropein and oleuropein aglycone were identified as deprotonated ions at m/z 539.06 and 377.12, respectively. Phase I metabolism was evidenced by the presence of elenolic acid (m/z 242.09), while extensive Phase II conjugation was indicated by the detection of elenolic acid glucuronide (m/z 407.20), hydroxytyrosol sulfate (m/z 279.07, formate adduct), hydroxytyrosol glucuronide (m/z 329.15), and hydroxytyrosol sulfo-glucuronide (m/z 409.24). Collectively, these findings indicate that rapid conjugation represents a dominant clearance pathway for oleuropein in plasma following oral administration.

Table 6. LC–MS detection of oleuropein metabolites in plasma. Metabolites identified in plasma are listed with their observed deprotonated molecular ions (m/z $[M-H]^-$) and corresponding formate adduct ions (m/z $[M^+HCOO]^-$) detected in negative electrospray ionization mode. Values represent experimentally observed masses used for metabolite confirmation.

Metabolite	m/z ([M−H])	m/z (Formate Adduct)
Oleuropein	539.06	585.19
Oleuropein Aglycone	377.12	-
Elenolic Acid-Glucuronide	407.2	453.21
Elenolic Acid (Free)	242.09	288.1
Hydroxytyrosol-Sulfate	-	279.07
Hydroxytyrosol-Glucuronide	329.15	-
Hydroxytyrosol-Sulfo-glucuronide	409.24	455.25

4. Discussion

The present study provides a report on the pharmacokinetic properties of oleuropein in C57BL/6 mice. In this study, we established an LC-MS/MS technique for measuring oleuropein and oleuropein aglycone, with both the analyte and internal standard measured in negative ion mode. Before sample analysis, the approach underwent a thorough validation process. The validation indicated that the established technique is accurate, precise, and reliable for the concurrent measurement of oleuropein and oleuropein aglycone. The performance parameters observed meet or exceed the acceptance requirements established by international guidelines for bioanalytical method validation, confirming the technique's suitability for its intended use. The analyte's elevated recovery rate and low variability (%RSD) indicate negligible matrix suppression or enhancement effects, as well as a very steady analytical response. This consistency is essential for producing dependable data, particularly at the lower limit of quantification, where elevated accuracy fosters significant confidence in assessing baseline concentrations.

The observed accuracy (mean values of 94.83–98.03%) and precision (RSDs of 6.73–13.62%) throughout the validation adhere to established bioanalytical standards, indicating no systematic bias and strong repeatability. This performance is underpinned by exceptional, consistent mean extraction recoveries of 94.79% and 95.85%, respectively. Moreover, the evaluation of matrix effects demonstrated that ion suppression or enhancement from mouse plasma components was minimal, as indicated by IS-normalized matrix factors remaining close to one. The significant analytical consistency across various plasma lots indicates that the intricate biological matrix did not impede analyte detection. These findings confirm the method's reliability and guarantee the quantitative precision of the given pharmacokinetic profiles.

The stability profile of a compound is essential for establishing standard operating procedures for sample handling and analysis. The excellent stability of oleuropein and oleuropein aglycone in the autosampler ensures that the processed samples may be reliably analyzed over a standard sequence run time without deterioration. The stability of both compounds at 4 °C, during long-term storage at −80 °C, and throughout multiple freeze–thaw cycles provides a strong basis for adaptable and efficient sample handling throughout the analytical process. This also underscores the need to avoid prolonged storage at elevated temperatures and that sample analysis must occur within a period that has demonstrated stability.

The metabolic stability of the analytes was significantly influenced by their chemical structure and the presence of enzymatic cofactors. In mouse liver microsomes, the determined CL_{int} for oleuropein aglycone was almost 14 times greater than that of its parent molecule, oleuropein, a pattern that persisted across the S9 fractions. The significant rise in clearance for the aglycone corroborates the anticipated high-velocity metabolic transitions identified during early characterization. The presence of the glycosidic moiety in oleuropein acts as a glucose shield, preventing the secoiridoid ring from opening into its highly reactive dialdehyde form, which is otherwise immediately susceptible to hepatic biotransformation [21,31]. Moreover, the activation of hepatic P450 systems through routes like peroxisome proliferator-activated receptor alpha (PPAR-α) activation may expedite the metabolism of these drugs in rodent models [32].

The in vivo pharmacokinetic profile in mice directly reflects the in vitro metabolic liability. After administering a 100 mg/kg oral dosage, oleuropein attained maximal plasma concentrations (C_{max}) in 30 min. The swift T_{max} suggests advantageous gastrointestinal permeability and closely corresponds with rodent studies demonstrating peak absorption of olive phenolics within 30 to 45 min [29,33]. Notwithstanding this effective absorption, the comparatively low systemic exposure and a brief metabolic half-life of roughly 0.78 h

suggest that oleuropein experiences significant intrinsic clearance. This swift systemic elimination is frequently opposed by extensive tissue distribution to the liver and heart, where it may provide localized protective effects [34,35].

The most striking finding was the total absence of quantifiable oleuropein aglycone in the plasma throughout the 24 h sampling period. Our data indicate that the conversion from oleuropein to its aglycone functions as a metabolic bottleneck. The aglycone's enhanced lipophilicity renders it an optimal substrate for nearly full presystemic metabolism, establishing a metabolic trap where it is biotransformed as rapidly as it is produced [23,34]. As a result, the aglycone experiences rapid first-pass metabolism through high-capacity UDP-glucuronosyltransferases (UGTs) and sulfotransferases (SULTs), preventing it from attaining prolonged systemic circulation. This elucidates why the glycosylated parent is transiently observable, whereas its more reactive aglycone remains below the quantification threshold [12,15,34].

The plasma metabolite profile provided definitive evidence that conjugative metabolism predominates in the disposition of oleuropein after absorption. The identification of Phase I metabolites such as elenolic acid, in conjunction with a comprehensive profile of Phase II conjugates including elenolic acid glucuronide, hydroxytyrosol glucuronide, and hydroxytyrosol sulfate, confirms substantial oxidative and hydrolytic processing. These findings reinforce the agreement that circulatory exposure predominantly consists of conjugated phenolic metabolites rather than solely the parent molecule [34,36]. From a translational standpoint, these findings underscore a critical disparity between the supplied dose of oleuropein and the molecular entities that ultimately engage with target tissues. The bioavailable portion predominantly comprises a complex mixture of glucuronides and sulfates; thus, any apparent biological activity should be interpreted as the cumulative effect of these metabolites. This metabolic intricacy indicates that further pharmacological models must consider metabolite exposure. Furthermore, it provides a strong rationale for developing delivery strategies or formulations designed to bypass pre-systemic metabolism, thereby enhancing the exposure of specific active forms like the aglycone.

Overall, these data demonstrate a definitive structure–metabolism relationship in which the glycosidic component of oleuropein is a crucial factor in metabolic stability, enabling quantifiable systemic exposure that is otherwise diminished following conversion to the aglycone. Integrating in vitro turnover rates with in vivo profiles reveals that although the oleuropein aglycone may exhibit greater theoretical potency, its swift Phase II biotransformation designates it as a temporary intermediate rather than a circulating bioactive compound. Consequently, oleuropein is identified as the principal entity relevant for oral administration. To comprehensively elucidate the kinetic profile of these phenolics, future intravenous studies are important; such data will facilitate the determination of absolute bioavailability and the differentiation of hepatic first-pass effects from systemic elimination. This differentiation is essential for creating precise exposure–response models and determining the exact dose-to-effect connections necessary for effective clinical translation.

Supplementary Materials: The following supporting information can be downloaded at: https://www.mdpi.com/article/10.3390/nutraceuticals6020024/s1. Table S1. Matrix effect assessment for oleuropein and oleuropein aglycone in mouse plasma. Table S2. Stability (%) of oleuropein and oleuropein aglycone at 4°C. Table S3. Stability (%) of oleuropein and oleuropein aglycone at −80°C. Table S4. Stability (%) of oleuropein and oleuropein aglycone at multiple freeze–thaw cycles. Table S5. Metabolic stability (%) of oleuropein and oleuropein aglycone in mouse liver microsomes with and without cofactors. Table S6. Metabolic stability (%) of oleuropein and oleuropein aglycone in S9 fractions with and without cofactors. Table S7. Intrinsic clearance (*CLint*) determination based on parent compound depletion during incubation.

Author Contributions: Conceptualization, P.S. and J.J.J.; methodology, P.S., P.T., R.R.R., and D.L.; validation, P.S.; formal analysis, P.S.; investigation, P.S., P.T., and R.R.R.; resources, J.J.J.; data curation, P.S.; writing—original draft preparation, P.S.; writing—review and editing, P.S., P.T., R.R.R., D.L., and J.J.J.; supervision, J.J.J.; project administration, J.J.J.; funding acquisition, J.J.J. All authors have read and agreed to the published version of the manuscript.

Funding: This research is supported by an NIH MERIT award (R37CA227101).

Institutional Review Board Statement: Animal experiments were performed according to the policies and guidelines of the Institutional Animal Care and Use Committee (IACUC) of the University of Illinois Chicago. Mice were euthanized in accordance with Institutional Animal Care and Use Committee approval (protocol 22-165; approved on 12 May 2022) and current AVMA guidelines (2020).

Informed Consent Statement: Not applicable.

Data Availability Statement: The original contributions presented in this study are included in the article and Supplementary Materials. Further inquiries can be directed to the corresponding author.

Conflicts of Interest: The authors declare no conflicts of interest.

Abbreviations

The following abbreviations are used in this manuscript:

ADME	Absorption, distribution, metabolism, and excretion
AUC	Area under the curve
C_{max}	Maximum observed plasma concentration
CV	Coefficient of variation
H-ESI	Heated electrospray ionization
HQ	High-quality control samples
IS	Internal standard
LDL	Low-density lipoprotein
LLOQ	Lower limit of quantification
LQ	Low-quality control sample
MQ	Medium-quality control sample
NAD(P)H	Nicotinamide adenine dinucleotide (phosphate), reduced form
PK	Pharmacokinetic
QC	Quality control
ROS	Reactive oxygen species
RPM	Revolutions per minute
RT	Room temperature
SOD	Superoxide dismutase
SRM	Selected reaction monitoring
T1/2	Terminal elimination half-life
T_{max}	Time at observed maximum concentration
UDPGA	Uridine 5′-diphosphate-glucuronic acid
UPLC-MS/MS	Ultra-performance liquid chromatography coupled with tandem mass spectrometry

References

1. de Lorgeril, M.; Salen, P.; Martin, J.-L.; Monjaud, I.; Delaye, J.; Mamelle, N. Mediterranean Diet, Traditional Risk Factors, and the Rate of Cardiovascular Complications After Myocardial Infarction. *Circulation* **1999**, *99*, 779–785. [CrossRef] [PubMed]
2. Dilis, V.; Katsoulis, M.; Lagiou, P.; Trichopoulos, D.; Naska, A.; Trichopoulou, A. Mediterranean diet and CHD: The Greek European Prospective Investigation into Cancer and Nutrition cohort. *Br. J. Nutr.* **2012**, *108*, 699–709. [CrossRef] [PubMed]
3. Cicerale, S.; Lucas, L.; Keast, R. Biological Activities of Phenolic Compounds Present in Virgin Olive Oil. *Int. J. Mol. Sci.* **2010**, *11*, 458–479. [CrossRef]
4. Omar, S.H. Oleuropein in Olive and its Pharmacological Effects. *Sci. Pharm.* **2010**, *78*, 133–154. [CrossRef]

5. Nediani, C.; Ruzzolini, J.; Romani, A.; Calorini, L. Oleuropein, a Bioactive Compound from *Olea europaea* L., as a Potential Preventive and Therapeutic Agent in Non-Communicable Diseases. *Antioxidants* **2019**, *8*, 578. [CrossRef]
6. Jemai, H.; Fki, I.; Bouaziz, M.; Bouallagui, Z.; El Feki, A.; Isoda, H.; Sayadi, S. Lipid-Lowering and Antioxidant Effects of Hydroxytyrosol and Its Triacetylated Derivative Recovered from Olive Tree Leaves in Cholesterol-Fed Rats. *J. Agric. Food Chem.* **2008**, *56*, 2630–2636. [CrossRef]
7. Manna, C.; Migliardi, V.; Golino, P.; Scognamiglio, A.; Galletti, P.; Chiariello, M.; Zappia, V. Oleuropein prevents oxidative myocardial injury induced by ischemia and reperfusion. *J. Nutr. Biochem.* **2004**, *15*, 461–466. [CrossRef] [PubMed]
8. Cumaoglu, A.; Rackova, L.; Stefek, M.; Kartal, M.; Maechler, P.; Karasu, C. Effects of olive leaf polyphenols against H_2O_2 toxicity in insulin secreting β-cells. *Acta Biochim. Pol.* **2011**, *58*, 45–50. [CrossRef]
9. Visioli, F.; Poli, A.; Gall, C. Antioxidant and other biological activities of phenols from olives and olive oil. *Med. Res. Rev.* **2002**, *22*, 65–75. [CrossRef]
10. Scoditti, E.; Calabriso, N.; Massaro, M.; Pellegrino, M.; Storelli, C.; Martines, G.; De Caterina, R.; Carluccio, M.A. Mediterranean diet polyphenols reduce inflammatory angiogenesis through MMP-9 and COX-2 inhibition in human vascular endothelial cells: A potentially protective mechanism in atherosclerotic vascular disease and cancer. *Arch. Biochem. Biophys.* **2012**, *527*, 81–89. [CrossRef]
11. Kim, Y.; Choi, Y.; Park, T. Hepatoprotective Effect of Oleuropein in Mice: Mechanisms Unveiled by Gene Expression Profiling. *Biotechnol. J.* **2018**, *13*, 1700505. [CrossRef]
12. Mahmoudi, A.; Hadrich, F.; Feki, I.; Ghorbel, H.; Bouallagui, Z.; Marrekchi, R.; Fourati, H.; Sayadi, S. Oleuropein and hydroxytyrosol rich extracts from olive leaves attenuate liver injury and lipid metabolism disturbance in bisphenol A-treated rats. *Food Funct.* **2018**, *9*, 3220–3234. [CrossRef]
13. Poudyal, H.; Campbell, F.; Brown, L. Olive leaf extract attenuates cardiac, hepatic, and metabolic changes in high carbohydrate, high fat-fed rats. *J. Nutr.* **2010**, *140*, 946–953. [CrossRef] [PubMed]
14. Hadrich, F.; Garcia, M.; Maalej, A.; Moldes, M.; Isoda, H.; Feve, B.; Sayadi, S. Oleuropein activated AMPK and induced insulin sensitivity in C2C12 muscle cells. *Life Sci.* **2016**, *151*, 167–173. [CrossRef]
15. de Bock, M.; Derraik, J.G.B.; Brennan, C.M.; Biggs, J.B.; Morgan, P.E.; Hodgkinson, S.C.; Hofman, P.L.; Cutfield, W.S. Olive (*Olea europaea* L.) Leaf Polyphenols Improve Insulin Sensitivity in Middle-Aged Overweight Men: A Randomized, Placebo-Controlled, Crossover Trial. *PLoS ONE* **2013**, *8*, e57622. [CrossRef]
16. Fujiwara, Y.; Tsukahara, C.; Ikeda, N.; Sone, Y.; Ishikawa, T.; Ichi, I.; Koike, T.; Aoki, Y. Oleuropein improves insulin resistance in skeletal muscle by promoting the translocation of GLUT4. *J. Clin. Biochem. Nutr.* **2017**, *61*, 196–202. [CrossRef] [PubMed]
17. Rigacci, S.; Miceli, C.; Nediani, C.; Berti, A.; Cascella, R.; Pantano, D.; Nardiello, P.; Luconi, M.; Raimondi, L.; Casamenti, F. Oleuropein aglycone induces autophagy via the AMPK/mTOR signalling pathway: A mechanistic insight. *Oncotarget* **2015**, *6*, 35344–35357.
18. Leri, M.; Oropesa-Nuñez, R.; Canale, C.; Raimondi, S.; Giorgetti, S.; Bruzzone, E.; Bellotti, V.; Stefani, M.; Bucciantini, M. Oleuropein aglycone: A polyphenol with different targets against amyloid toxicity. *Biochim. Biophys. Acta Gen. Subj.* **2018**, *1862*, 1432–1442. [CrossRef] [PubMed]
19. Galiano, V.; Villalaín, J. Oleuropein aglycone in lipid bilayer membranes. A molecular dynamics study. *Biochim. Biophys. Acta Biomembr.* **2015**, *1848*, 2849–2858. [CrossRef] [PubMed]
20. Gutiérrez-Rosales, F.; Romero, M.; Casanovas, M.; Motilva, M.; Mínguez-Mosquera, M. Metabolites involved in oleuropein accumulation and degradation in fruits of *Olea europaea* L.: Hojiblanca and Arbequina varieties. *J. Agric. Food Chem.* **2010**, *58*, 12924–12933. [CrossRef]
21. de Bock, M.D.; Thorstensen, E.; Derraik, J.G.; Henderson, H.V.; Hofman, P.L.; Cutfield, W.S. Human absorption and metabolism of oleuropein and hydroxytyrosol ingested as olive (*Olea europaea* L.) leaf extract. *Mol. Nutr. Food Res.* **2013**, *57*, 2079–2085. [CrossRef]
22. Galmés, S.; Reynés, B.; Palou, M.; Palou-March, A.; Palou, A. Absorption, Distribution, Metabolism, and Excretion of the Main Olive Tree Phenols and Polyphenols: A Literature Review. *J. Agric. Food Chem.* **2021**, *69*, 5281–5296. [CrossRef]
23. Nikou, T.; Sakavitsi, M.; Kalampokis, E.; Halabalaki, M. Metabolism and Bioavailability of Olive Bioactive Constituents Based on In Vitro, In Vivo and Human Studies. *Nutrients* **2022**, *14*, 3773. [CrossRef]
24. Corona, G.; Tzounis, X.; Dessì, M.A.; Deiana, M.; Debnam, E.S.; Visioli, F.; Jeremy, J.P. The fate of olive oil polyphenols in the gastrointestinal tract: Implications of gastric and colonic microflora-dependent biotransformation. *Free Radical Res.* **2006**, *40*, 647–658. [CrossRef] [PubMed]
25. Rocchetti, G.; Senizza, B.; Giuberti, G.; Montesano, D.; Trevisan, M.; Lucini, L. Metabolomic Study to Evaluate the Transformations of Extra-Virgin Olive Oil's Antioxidant Phytochemicals During In Vitro Gastrointestinal Digestion. *Antioxidants* **2020**, *9*, 302. [CrossRef]
26. de la Torre, R. Bioavailability of olive oil phenolic compounds in humans. *Inflammopharmacology* **2008**, *16*, 245–251. [CrossRef] [PubMed]

27. Luque-Muñoz, A.; Tapia, R.; Haidour, A.; Justicia, J.; Cuerva, J.M. Direct determination of phenolic secoiridoids in olive oil by ultra-high performance liquid chromatography-triple quadruple mass spectrometry analysis. *Sci. Rep.* **2019**, *9*, 15545. [CrossRef]
28. Celano, R.; Piccinelli, A.L.; Pugliese, A.; Carabetta, S.; Di Sanzo, R.; Russo, M.; Rastrelli, L. Insights into the Analysis of Phenolic Secoiridoids in Extra Virgin Olive Oil. *J. Agric. Food Chem.* **2018**, *66*, 6053–6063. [CrossRef]
29. Bazoti, F.N.; Gikas, E.; Tsarbopoulos, A. Simultaneous quantification of oleuropein and its metabolites in rat plasma by liquid chromatography electrospray ionization tandem mass spectrometry. *Biomed. Chromatogr.* **2010**, *24*, 506–515. [PubMed]
30. Del Boccio, P.; Di Deo, A.; De Curtis, A.; Celli, N.; Iacoviello, L.; Rotilio, D. Liquid chromatography-tandem mass spectrometry analysis of oleuropein and its metabolite hydroxytyrosol in rat plasma and urine after oral administration. *J. Chromatogr. B* **2003**, *785*, 47–56. [CrossRef]
31. Gentile, L.; Uccella, N.; Sivakumar, G. Oleuropein: Molecular Dynamics and Computation. *Curr. Med. Chem.* **2017**, *24*, 4315–4328. [CrossRef] [PubMed]
32. Malliou, F.; Andriopoulou, C.E.; Gonzalez, F.; Kofinas, A.; Skaltsounis, A.-L.; Konstandi, M. Oleuropein-Induced Acceleration of Cytochrome P450-Catalyzed Drug Metabolism: Central Role for Nuclear Receptor Peroxisome Proliferator-Activated Receptor alpha. *Drug Metab. Dispos.* **2021**, *49*, 833–843. [CrossRef] [PubMed]
33. Kundisová, I.; Colom, H.; Juan, M.; Planas, J.M. Pharmacokinetics of Hydroxytyrosol and Its Sulfate and Glucuronide Metabolites after the Oral Administration of Table Olives to Sprague-Dawley Rats. *J. Agric. Food Chem.* **2024**, *72*, 2154–2164. [CrossRef] [PubMed]
34. Serra, A.; Rubió, L.; Borràs, X.; Macià, A.; Romero, M.; Motilva, M. Distribution of olive oil phenolic compounds in rat tissues after administration of a phenolic extract from olive cake. *Mol. Nutr. Food Res.* **2012**, *56*, 486–496. Erratum in *Mol. Nutr. Food Res.* **2012**, *56*, 1185.
35. Potočnjak, I.; Škoda, M.; Pernjak-Pugel, E.; Peršić, M.P.; Domitrović, R. Oral administration of oleuropein attenuates cisplatin-induced acute renal injury in mice through inhibition of ERK signaling. *Mol. Nutr. Food Res.* **2016**, *60*, 530–541. [CrossRef]
36. Alemán-Jiménez, C.; Domínguez-Perles, R.; Medina, S.; Prgomet, I.; López-González, I.; Simonelli-Muñoz, A.; Campillo-Cano, M.; Auñón, D.; Ferreres, F.; Gil-Izquierdo, Á. Pharmacokinetics and bioavailability of hydroxytyrosol are dependent on the food matrix in humans. *Eur. J. Nutr.* **2021**, *60*, 905–915.